

Proposal; Precise measurements of very forward particle production at RHIC

Y.Itow, H.Menjo, T.Sako, N.Sakurai

Solar-Terrestrial Environment Laboratory / Kobayashi-Maskawa Institute for the Origin of Particles and the Universe / Graduate School of Science, Nagoya University, Japan

K.Kasahara, T.Suzuki, S.Torii

Waseda University, Japan

O.Adriani, L.Bonechi, R.D'Alessandro, G.Mitsuka, A.Tricomi

INFN/University of Firenze/University of Catania, Italy

Y.Goto

RIKEN Nishina Center / RIKEN BNL Research Center, Japan

K.Tanida

Seoul National University

ABSTRACT

We propose a new experiment Relativistic Heavy Ion Collider forward (RHICf) for the precise measurements of very forward particle production at RHIC. The proposal is to install the LHCf Arm2 detector in the North side of the ZDC installation slot at the PHENIX interaction point. By installing high-resolution electromagnetic calorimeters at this location we can measure the spectra of photons, neutrons and π^0 at pseudorapidity $\eta > 6$.

The new measurements at 510 GeV p+p collisions contribute to improve the hadronic interaction models used in the cosmic-ray air shower simulations. Using a kinematic coverage at RHIC similar to that of the measurements at LHC 7–14 TeV p+p collisions, we can test the scaling of forward particle spectra with a wide \sqrt{s} range and make the extrapolation of models into cosmic-ray energy more reliable. Combination of a high position resolution of the RHICf detector and a high energy resolution of the ZDC makes it possible to determine p_T of forward neutrons with the ever best resolution. This enables us to study the forward neutron spin asymmetry discovered at RHIC in more detail. Combined data taking and analysis between PHENIX and RHICf will make it possible to identify the origin of each forward particle, particularly diffractive and non-diffractive interactions.

We request 510 GeV p+p collisions with $\beta^*=10$ m. With 100 and 20 colliding and non-colliding bunches, respectively, and nominal bunch intensity 2×10^{11} , we can expect an instantaneous luminosity of $1.1 \times 10^{31} \text{ cm}^{-2} \text{ s}^{-1}$. To study the asymmetry of forward particle production, we require radially polarized beams with a moderate polarization, 0.4-0.5 or higher. These beam conditions provide sufficient event statistics after one day of operation. Including another day for contingency and 1-5 days for beam setup depending on the previous beam mode, we propose 3-7 days of beam time to complete our proposal.

RHICf is also interested in participating a possible measurements at p+A collisions to understand the interaction between cosmic-ray particles and atmosphere. Collision of light ions like nitrogen is the ultimate goal for the cosmic-ray physics, but the collision of heavy ion is also of interest.

Our proposal is to bring the LHCf Arm2 detector to RHIC after the LHC 13 TeV p+p collision runs planned in early 2015, and then operate in RUN16 at RHIC. Installation of the cables and a structure to fix the detector, preparation for the data acquisition especially synchronization with PHENIX and accelerator will be carried out in advance as soon as the proposal is approved.

Contents

1	Introduction and physics	4
1.1	Cosmic-ray physics and \sqrt{s} dependence of hadronic interaction	4
1.2	Asymmetry in the forward particle production in the polarized p+p collisions	5
1.3	LHCf experiment	6
2	Experimental setup and detector	9
2.1	LHCf detector at RHIC	9
2.2	Data acquisition	10
2.3	Joint operation with PHENIX	12
3	Beam conditions and operation scenario	17
3.1	Beam conditions and setup time	17
3.2	Operation scenario with 510 GeV p+p collisions	19
4	Expected results	21
4.1	Single particle spectra	21
4.2	π^0 spectra	21
4.3	Spin asymmetry	22
5	Schedule and expected supports from BNL	27
5.1	Schedule	27
5.2	Expected supports from BNL	28
6	Manpower and budget	29

Chapter 1

Introduction and physics

1.1 Cosmic-ray physics and \sqrt{s} dependence of hadronic interaction

The origin of cosmic rays is a century-standing problem. Recent observations of ultra-high-energy cosmic rays (UHECR) by the Pierre Auger Observatory (PAO) [1] and Telescope Array [2] have been dramatically improved in both the statistics and the systematics. The existence of a spectral cutoff at approximately $10^{19.5}$ eV is now clearly identified. However, the interpretation of the observed results is not settled. One of the main reasons for the difficulty is the uncertainty in air shower modeling. Fig.1.1 shows the so-called X_{max} parameter as a function of the cosmic-ray energy observed by the PAO. Here, X_{max} is the height of the shower maximum measured from the top of the atmosphere in g/cm^2 . Experimental data are compared with the predictions by air shower simulation with the two extreme assumptions that all cosmic rays are protons or iron nuclei. Four lines in each assumption are due to the use of different interaction models in the air shower simulation. Because of the fact that the difference between models is larger than the experimental errors, the determination of the primary chemical composition is difficult, and hence, the nature of the spectral cutoff is not concluded. The determination of the chemical composition at 10^{17} eV is also important because, at approximately this energy, the source of the cosmic rays is believed to switch from galactic to extragalactic and the chemical composition rapidly changes with energy [3]. However, due to the uncertainty in air shower modeling, the determination of the chemical composition at this energy range is still model dependent. To solve the origin of mysterious UHECRs and to confirm the standard scenario of the cosmic-ray origin, constraints from the accelerator experiments are indispensable.

The difficulty in modeling hadronic interactions, which is essential to determine the air shower development, is due to the difficulty in modeling the soft interaction described by non-perturbative QCD. Experimentally, particles produced in such processes have a large energy flux in the forward direction and are difficult to measure especially in collider experiments. Cosmic-ray interaction models have been tested with a variety of accelerator experiments with a limited number of forward measure-

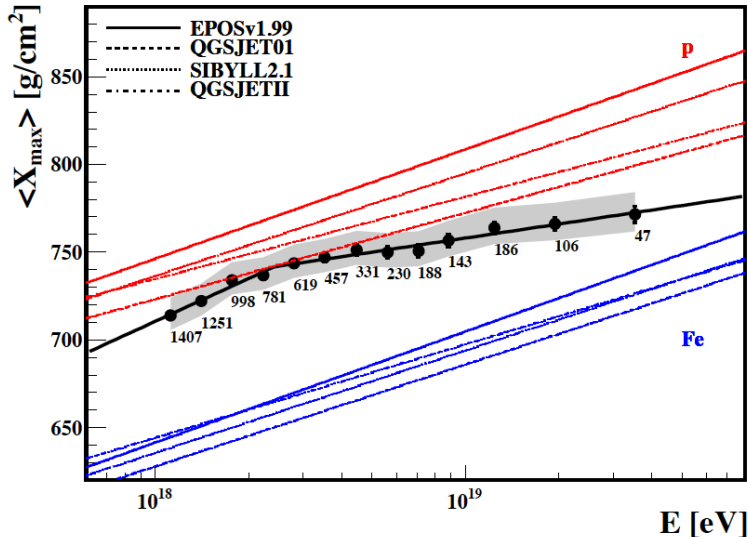


Figure 1.1: X_{max} of air showers observed by the Pierre Auger Observatory. [1]

ments, and most of the data thus far are limited in proton-proton (or anti-proton) collisions. The Large Hadron Collider (LHC) provides an unprecedented quality of test data; this facility gives the highest collision energy, and the experiments cover a very wide range of pseudorapidity (η) [4]. The same quality of lower-energy collision data is very important to test the \sqrt{s} dependence of hadronic interactions to extrapolate the models beyond the LHC energy. Fig.1.2 shows the energy spectra of all π^0 at $\sqrt{s}=500$ GeV, 7 TeV and 50 TeV ($E_{lab}=1.3 \times 10^{18}$ eV) predicted by the DPMJET3 [5] and QGSJET-II [6] models. With the particle energy scaled by the beam energy (x_F), the DPMJET3 model assumes a perfect scaling, whereas QGSJET-II shows a softening in higher energy collisions. The assumption of the scaling or collision energy dependence is an important issue to be tested at the collider experiments.

In contrast to p+p collisions, only d+Au collisions at RHIC and p+Pb collisions at LHC have provided collision situations that are similar to cosmic-ray protons interacting with the atmosphere. In both cases, strong nuclear effects were reported by STAR [7] and ALICE [8]. These effects will be important inputs to simulate proton-atmosphere collisions at extreme conditions. However, no direct tests of nuclear effects in proton-atmosphere collisions have been performed thus far.

1.2 Asymmetry in the forward particle production in the polarized p+p collisions

With the first polarized p+p collisions at $\sqrt{s}=200$ GeV at RHIC, a large single transverse-spin asymmetry (A_N) for neutron production in very forward kinematics was discovered by a polarimeter development experiment [9]. This was recently

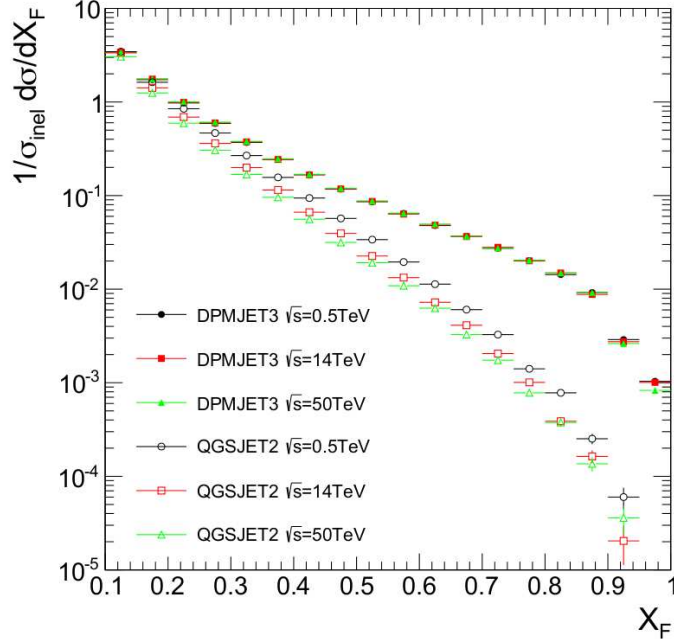


Figure 1.2: X_F spectra of all π^0 at $\sqrt{s} = 500$ GeV, 7 TeV and 50 TeV p+p collisions.

confirmed by the PHENIX experiment using the Zero Degree Calorimeter (ZDC) and the Shower Maximum Detector (SMD) installed between the ZDC modules [10]. The discovery of the large A_N for neutron production is new, important information to understand the production mechanism of the very forward neutron.

The \sqrt{s} dependence of A_N from three different collision energies, 62.4 GeV, 200 GeV, and 500 GeV was studied [11]. The result is shown in Fig. 1.3. The hit position dependence on the detector was measured at each energy, although this dependence was largely smeared by the position resolution. The result was converted to the p_T dependence, which showed a hint of the p_T scaling property of A_N of the very forward neutron production. The asymmetry is caused by interference between spin-flip and non-flip amplitudes with a relative phase. Kopeliovich et al. [12] studied the interference of a pion and a_1 , or a pion and ρ in the 1^+S state. The data agreed well with the independence of energy. The asymmetry is sensitive to the presence of different mechanisms, e.g., Reggeon exchange with spin-non-flip amplitudes, in addition to the dominant one-pion exchange amplitude, even if these amplitudes are small.

1.3 LHCf experiment

Large Hadron Collider forward (LHCf) is one of the LHC experiments to measure forward neutral particles to calibrate the interaction models used in the cosmic-ray physics [13]. LHCf successfully acquired to take data for LHC 900 GeV, 2.76 TeV and

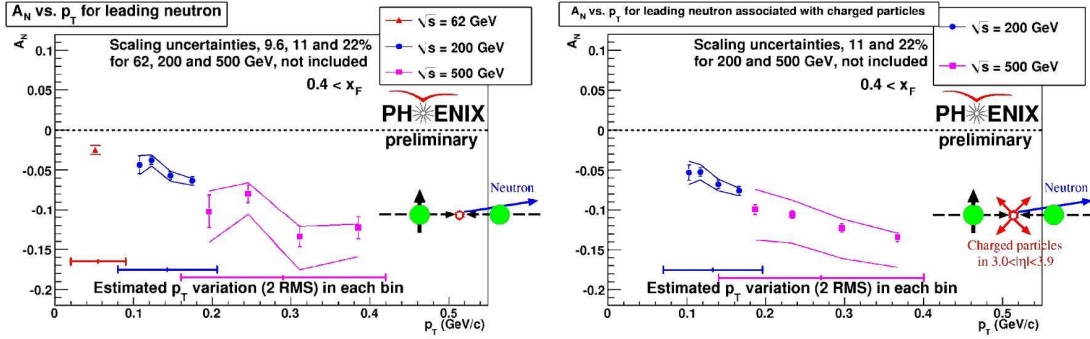


Figure 1.3: The measured asymmetries of very forward neutron production as functions of p_T with an inclusive-neutron trigger (left) and with a semi-inclusive neutron trigger including a beam-beam interaction requirement (right).

7 TeV p+p collisions and 5.0 TeV ($\sqrt{s_{NN}}$) p+Pb collisions. LHCf installed compact calorimeters at the installation slots of the ZDCs located 140 m from an interaction point of the LHC. Two independent detectors called Arm1 and Arm2 at either side of the interaction point were installed. At this location, neutral particles (predominantly photons decayed from π^0 and neutrons) emitted at $\eta > 8.4$ are observed. Each detector has two small calorimeter towers that allow simultaneous detection of two high-energy particles and hence identification of photon pairs originating from π^0 by reconstructing the invariant mass of these particles. The performance of the detectors at LHC was satisfactory and well understood [14]. LHCf is preparing for measurements at LHC 13 TeV p+p collisions in April to May, 2015.

Thus far, LHCf has published energy spectra of forward photons at 900 GeV [15] and 7 TeV [16] and forward π^0 spectra at 7 TeV [17]. The suppression of forward π^0 production in the p+Pb collisions was also reported recently [18]. As mentioned above, comparisons of data at different collision energies are extremely important. Fig.1.4 shows a MC prediction of forward photon yield ($\frac{d^2N}{N_0 dx_F dp_T}$). In a model characterized by perfect scaling this distribution is \sqrt{s} independent. The triangles in the figure indicate the phase-space coverages with LHC set at 900 GeV and 7 TeV, and also with RHIC set at 200 GeV and 500 GeV. It is found that the LHC 7 TeV and RHIC 500 GeV settings cover an almost identical phase space, while the other operating points have different and very limited phase-space coverages. The prime motivation for RHICf is to measure the forward particles production with identical phase-space coverages and test the \sqrt{s} scaling.

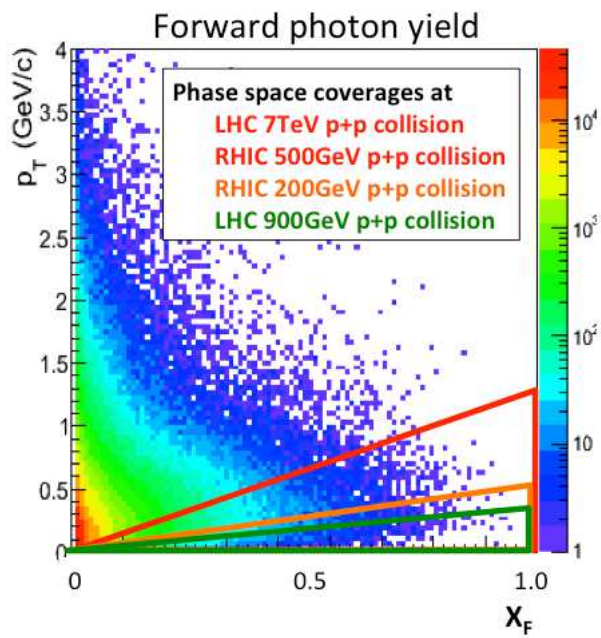


Figure 1.4: Comparison of phase space coverages of photons between LHCf and RHICf.

Chapter 2

Experimental setup and detector

2.1 LHCf detector at RHIC

The idea at the basis of the RHICf proposal is to bring one of the LHCf detectors [19] [20] called Arm2 shown in Fig.2.1 to RHIC and to install it in front of a ZDC at the interaction point of the PHENIX experiment. The LHCf Arm2 detector, called the RHICf detector hereafter, is composed of two sampling calorimeter towers with transverse dimensions to the beam of $25\text{ mm}\times 25\text{ mm}$ and $32\text{ mm}\times 32\text{ mm}$. Each tower is composed of 44 radiation lengths of Tungsten interleaved with 16 scintillator layers. Signals from scintillators are measured by 32 PMTs (HAMAMATSU R7400U). Eight layers (4 XY pairs) of silicon strip sensors are inserted to measure the lateral distribution of the showers. The calorimeters have an energy and a position resolutions of $8\%/\sqrt{E/100\text{ GeV}}+1\%$ and $<150\text{ }\mu\text{m}$ ($>50\text{ GeV}$), respectively, for electromagnetic showers in the LHC environment. The detector is contained in an aluminum box with the dimensions of 92 mm (transverse to the beam direction) \times 290 mm (along the beam) \times 620 mm in height. This can fit the 100 mm gap between the beam pipes located at 18 m from the interaction point of RHIC where ZDCs are located. By installing the RHICf detector in front of a ZDC at the PHENIX interaction point, RHICf measures the neutral particles around zero degree. The location of the installation is supposed at the North side of PHENIX due to the available space at the time of May 2014 and to keep a possibility of observing from the proton remnant side in p+A collisions.

The RHICf detector will be suspended from a structure called manipulator that allows a vertical movement of the detector. The purposes of the manipulator are 1) to increase the rapidity (or p_T) coverage, 2) to avoid interference to ZDC running when RHICf is not in operation. At the location of ZDC neutral particles are detectable up to the radius $r=100\text{ mm}$ or $\eta=6$. On the other hand, because of the transverse sizes of the RHICf calorimeters, the accessible phase space is not covered all at once. A possible pattern of the vertical scan positions, their coverage in the p_T - x_F plane and acceptance for different categories of events are summarized in Fig.2.2, Fig.2.3 and Tab.2.1. Acceptance is defined as an expected number of events in an inelastic collision calculated based on the generator PYTHIA 8.185 [21].

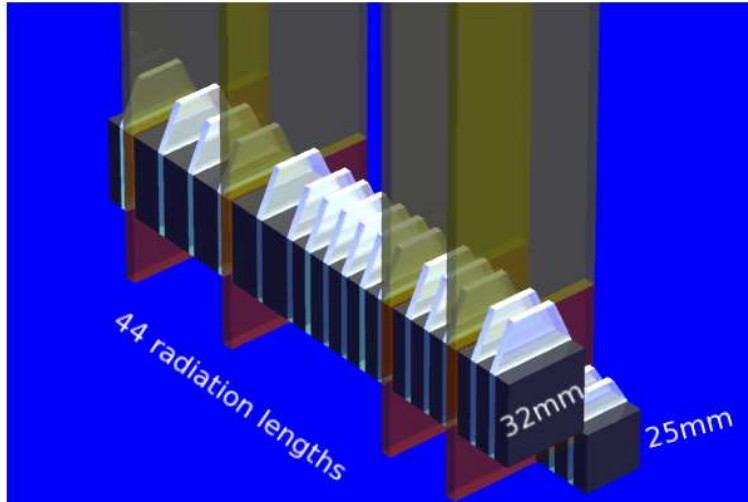


Figure 2.1: Schematic view of the RHICf detector.

Together with the manipulator, the detector is installed with the front-end circuit of the silicon strip sensors and the PMT preamplifiers. All components were assembled on a single aluminum plate and installed in the LHC tunnel when they were used in the LHCf experiment as shown in Fig.2.4. Fig.2.5 shows a photograph when the detector and electronics were fixed on the TAN radiation shield (red part in photo) in the LHC tunnel. RHICf needs the same identical components except for the manipulator that must be upgraded to allow a wider movable range at RHIC. Conceptual images showing how the RHICf detector and its electronics will be installed in the RHIC tunnel are shown in Fig.2.6. Left figure shows the beam pipes (grey), RHICf (blue) and ZDC (magenta) while right figure includes the manipulator and the electronics (green) and their support structure (yellow). It is necessary to construct the structure to hold the RHICf equipment which weighs about 80 kg in total.

2.2 Data acquisition

RHICf records the signals from 32 PMTs for the calorimeters and from 3,072 silicon strips (3 clock samples for each strip). The signals from the silicon strip sensors are digitized near the detector and transferred to the rack room through optical fibers. The $3\ \mu\text{sec}$ deep analog pipeline of the silicon readout was designed to work with the 40 MHz LHC clock, but it is confirmed that it is also operational at 37.7 MHz corresponding to $4\times$ (RHIC clock). On the other hand, the analog signals from PMTs are amplified and transferred to the rack room through coaxial cables. The charge from the PMTs are recorded by charge ADCs (CAEN V965) through a conventional technique; linear fanout, discriminators (CAEN V814) and analog delay cables. The discriminator outputs are sent to a FPGA module and a trigger signal is issued when

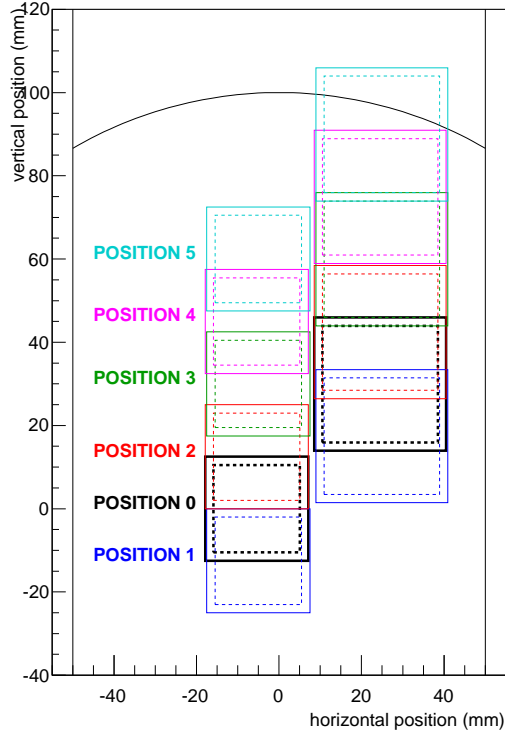


Figure 2.2: Candidate scan positions. The origin is defined at the zero degree or $\eta=\infty$. The arc at the top indicates the observation limit, $\eta=6$, constrained by the narrowest beam pipe. Small and large squares indicate the coverage of the 25 mm and 32 mm calorimeters, respectively. Dashed squares indicate the fiducial area used in the standard LHCf analysis.

an existence of a high-energy shower is identified. A time chart of the signal processing is outlined in Fig.2.7. To synchronize with the collisions a signal synchronized with each bunch (spin flag signals, for example) and a clock signal provided by the RHIC machine are required.

The space for installing the electronics could be provided by the PHENIX group in the PHENIX rack room and also about 50 cables (30–80 meters long) must be installed. The length of the cables depends on whether they will follow the standard path or whether a short cut to the rack room can be used. Some power supplies will be installed near the detector where it is shielded from radiation and some electronics are already in operation. The length of the cables from the detector to the power supplies is supposed to be 10 m. A list of necessary cables and a schematic diagram are shown in Tab.2.2 and Fig.2.8. More detail investigation of the cabling will be discussed in 2014 summer after RUN14.

Constraints in the event rate

The data recording in the rack room is carried out through VME bus. This limits the speed of the RHICf data acquisition to 1 kHz and results in a large inefficiency at high luminosity. Not only the inefficiency but signal overlap causes problems

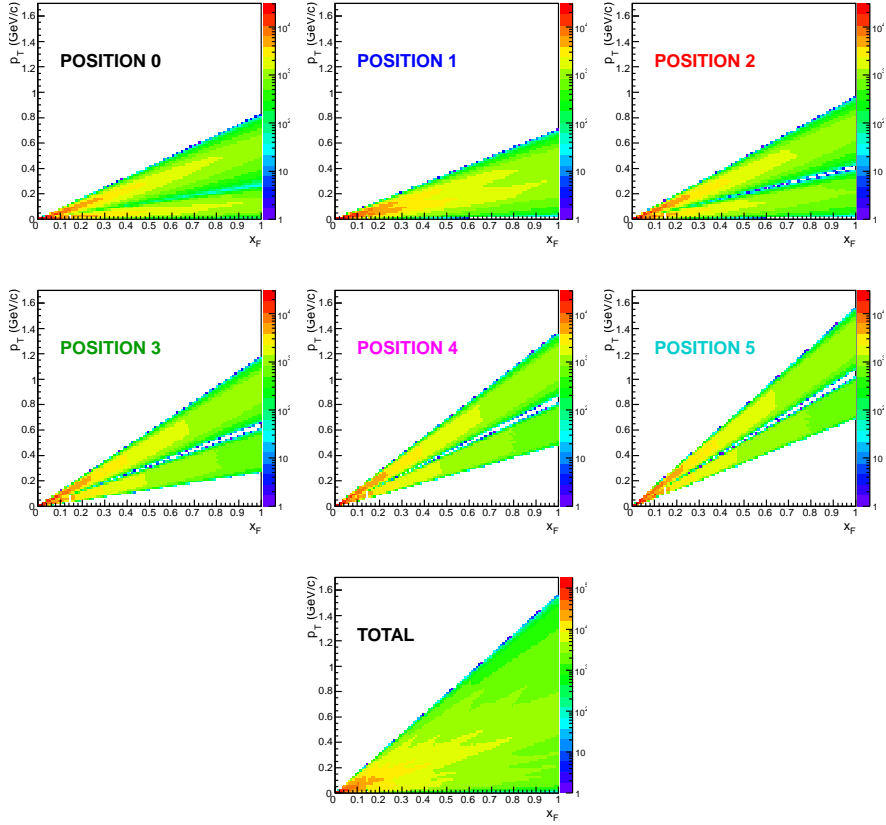


Figure 2.3: Coverage in the p_T - x_F plane for 6 scanning positions given in the Fig.2.2 and a sum of them at the bottom. The color represents the effective fiducial area of the calorimeters in log scale.

at high luminosity. The RHICf calorimeters use Gd_2SiO_5 (GSO) scintillators to avoid radiation damage during LHC operation. The slow decay constant of the GSO scintillators was also important to avoid a saturation of the PMTs at LHC. The slow decay constant, however, causes an overlap of signals when successive events occur within a short time interval. For safety, $10 \mu\text{sec}$ is assumed when we discuss about the beam condition and operation plan in Chapter.3.

2.3 Joint operation with PHENIX

Recording the events from identical collisions between PHENIX and RHICf will open a new possibility for the collider experiments. 1) This joint analysis enables a similar analysis to the one carried out by PHENIX ZDC+SMD and BBC for spin asymmetry measurement. 2) As discussed in our LOI [22], joint analysis of RHICf and PHENIX ZDC will improve the p_T resolution for forward neutrons. 3) Correlation between the very forward detector and the central detector will provide new information about

Table 2.1: Acceptance of RHICf detector for 6 positions and deferent event categories. Acceptance is defined as 'event/inelastic collision' using PYTHIA 8.185. Fiducial cut in the standard LHCf analysis is applied. Energy thresholds of 30 GeV and 100% detection efficiency were assumed. TS and TL designate Small Tower (calorimeter) and Large Tower, respectively.

Position	All event	photon		neutron		π^0
		TS	TL	TS	TL	
0	0.047	0.0079	0.011	0.014	0.014	0.00023
1	0.049	0.0077	0.012	0.013	0.016	0.00025
2	0.043	0.0077	0.010	0.013	0.012	0.00020
3	0.034	0.0069	0.0087	0.0094	0.0086	0.00015
4	0.027	0.0060	0.0074	0.0071	0.0067	0.00011
5	0.019	0.0052	0.0047	0.0054	0.0039	0.00006

low mass diffraction events. 4) Should RHICf can operate during p+A collisions, information from the central detector is useful to estimate impact parameter of each collision. 5) In p+A collisions, information from the central detector is useful to extract the events from Ultra Peripheral Collisions that was observed by LHCf in the p+Pb collisions [18].

The current idea of PHENIX-RHICf joint operation is to trigger PHENIX according to the RHICf trigger signals. As shown in the time chart in Fig.2.7, RHICf can decide to record data after about 500 ns from a collision. Using this signal, PHENIX has enough time to record the data for the same event. Because the maximum PHENIX DAQ speed is 5 kHz while it is 1 kHz for RHICf, PHENIX is in principle able to record all of the RHICf triggered events. Usage of PHENIX trigger signals for the RHICf trigger is also under consideration. To ensure offline event identification between two experiments, RHICf will record the clock counter signal provided by PHENIX. This counter is an accumulated count of 10 MHz clock with a 64-bit dynamic range, thus provides an absolute time for each event.

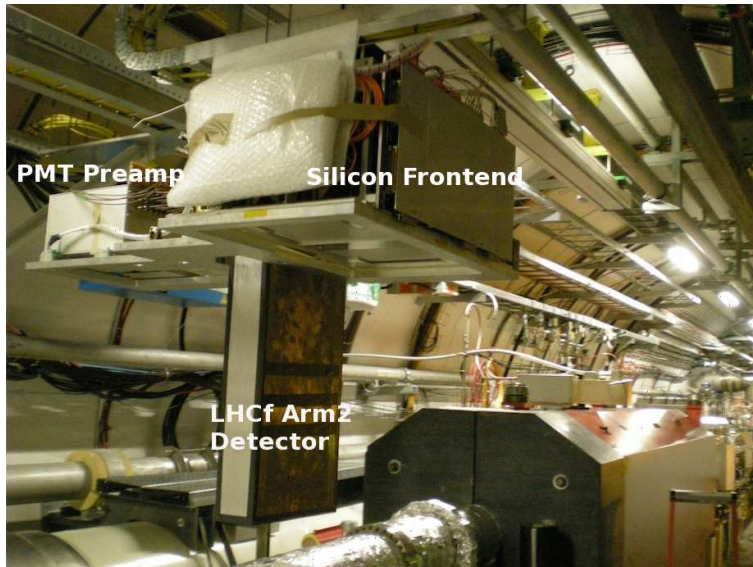


Figure 2.4: The LHCf Arm2 detector and its fronted electronics during the installation in the LHC tunnel.

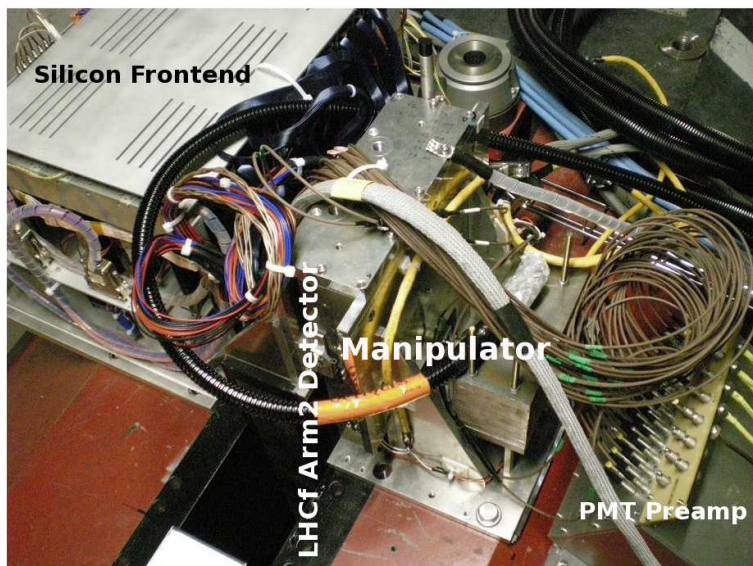


Figure 2.5: The LHCf Arm2 detector and its fronted electronics fixed on the TAN.

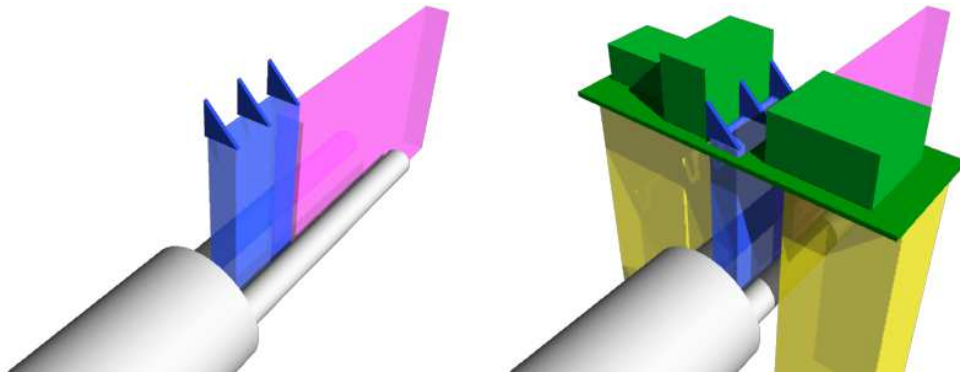


Figure 2.6: The LHCf Arm2 detector and its fronted electronics fixed on the TAN.

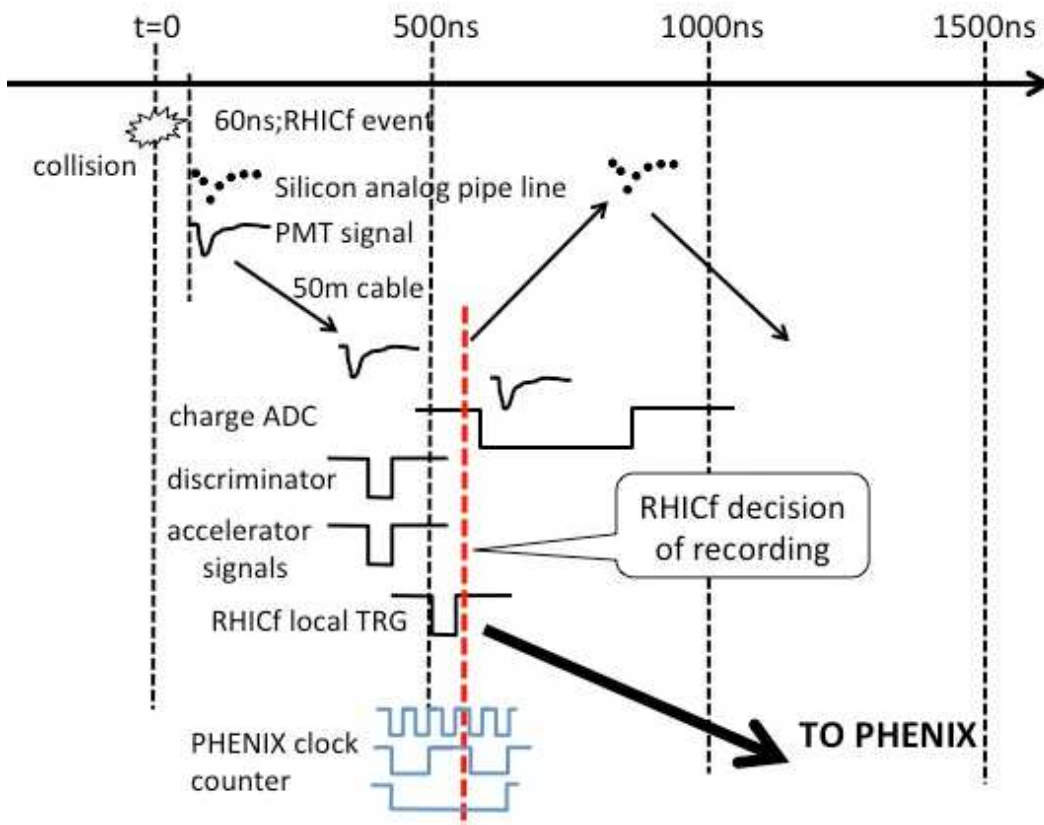


Figure 2.7: Time chart of the RHICf data acquisition.

Table 2.2: List of cables between the detector and the rack room (long cables), between the detector and the power supplies (short cables).

Type (connector)	Quantity	Purpose
[Long cables]		
50Ω coaxial (BNC)	32+10	PMT signal, encoder
25 wires low current (DSUB)	3	Sensors (ex. T mon)
Optical fiber bundle (16 single mode; custom made)	2	Silicon control
Optical fiber (multi mode)	6	Silicon readout
Optical fiber	1	PMT calibration
[Short cables]		
37 wires HV (1000V; REDEL)	1	PMT HV
16 wires MV (100V)	1	Silicon bias
2 wires high current (<10A)	16	Silicon frontend
3 wires mid current (<3A)	1	Manipulator drive
2 wires low current (<1A)	16	Silicon FE sensors
16 wires low current (<1A)	1	Silicon bias sensors

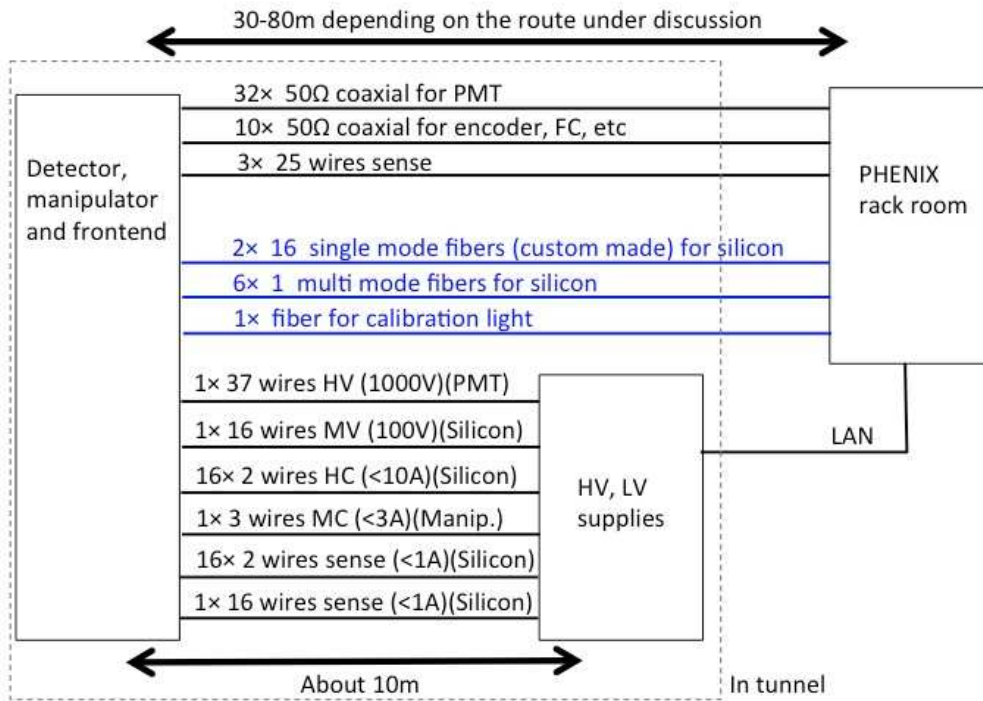


Figure 2.8: Plan of cabling between the RHICf detector and the PHENIX rack room.

Chapter 3

Beam conditions and operation scenario

3.1 Beam conditions and setup time

To obtain a wide p_T coverage comparable to the LHCf measurements, operation at 510 GeV p+p collisions is our target. To avoid an angular divergence, a high β^* is needed. Assuming a nominal emittance $\epsilon^*=20$ mm mrad and $\beta^*=10$ m, $86 \mu\text{rad}$ of angular dispersion is expected. This results in a 1.5 mm dispersion at the RHICf distance which is compatible with our physics goal.

Due to the high β^* , luminosity becomes reasonably low even with a nominal bunch intensity $I_b=2\times 10^{11}$. With 100 collision bunches the total luminosity and collision pileup (μ) are $1.1\times 10^{31} \text{ cm}^{-2}\text{s}^{-1}$ and 6.5%, respectively. Insertion of about 20 non-colliding bunches is necessary to study the background from beam halo and interaction between the beam and residual gas in the vacuum chamber. Considering the maximum RHICf acceptance, 0.05, in Tab.2.1, and the inelastic cross section $\sigma_{ine}=50$ mb, the RHICf event rate will be 28 kHz though the recording rate will be limited to 1 kHz because of the aforementioned DAQ limits. Prescaling of the single calorimeter events down to <1 kHz while recording all double calorimeter events will be applied to enhance the relatively low rate of π^0 events (140 Hz at position 1). Also enhanced triggers for high energy showers and a rough classification between electromagnetic and hadronic showers are possible. According to the largest acceptance of a single calorimeter (0.012+0.016 for the Large Tower at the position 1 in Tab.2.1), the fraction of multiple shower events in a single calorimeter due to the collision pileup is 0.2% (0.065×0.028) at maximum and is at an acceptable level. The probability that successive events occur within $10 \mu\text{sec}$ is 15%. These events may deteriorate the charge measurement of the calorimeters due to the slow GSO decay time, but they can be identified and eliminated in the analysis.

To study single spin asymmetry of the forward particle production, we require a polarized p+p collision. Since RHICf can perform scans by moving its position only in the vertical direction, radial polarization resulting an up-down asymmetry is required. Mixture of alternating polarization directions is important to reduce

Table 3.1: Required beam parameters for 510 GeV p+p collision.

Parameter	Value
Beam energy (GeV)	255
Beam intensity (protons per bunch)	2×10^{11}
Number of colliding bunch	100
Number of non-colliding bunch	20
Beam emittance (mm mrad)	20
β^* (m)	10
Luminosity ($\text{cm}^{-2}\text{s}^{-1}$)	1.1×10^{31}
Polarization direction	radial
Polarization amplitude	0.4–0.5
Operation time	1 day

systematic uncertainty. Reasonably high polarization, 0.4–0.5, is required. Any higher polarization is always appreciated.

The required beam parameters for the RHICf operation are summarized in Tab.3.1. They were also studied by the CA-D section and summarized in the ‘RHIC Collider Projection (FY2014–FY2018) version 6 April 2014 [23].’ According to [23], the expected setup time for the RHICf requested beam conditions are given depending on the previous beam mode.

- Previous mode: polarized protons at the same energy
 - 1 day of setup is needed
 - expected polarization is the same as in the previous running mode
- Previous mode: polarized protons at different energy
 - 2 days of setup are needed
 - some reduction in the proton intensity per bunch
 - expected polarization at 255 GeV is up to 55%
- Previous mode: heavy ions
 - 4-5 days of setup are needed
 - reduction in the proton intensity per bunch by up to 30%
 - expected polarization at 255 GeV is up to 50%
 - since the polarimeters also need commissioning time, the polarization measurements will have a large error

Therefore RHICf operation at the end of 510 GeV polarized p+p collision program is strongly preferred.

3.2 Operation scenario with 510 GeV p+p collisions

A schedule before RUN16 will be described in Chap.5. Once beam operation starts, RHICf will wait for its operation time at the garage position defined as the highest position within reach of the manipulator. Even at this position, particles produced in the collisions will anyway arrive at the detector after interacting with the beam pipe. Using these background particles, tuning of the electronics, mainly timing synchronization with collision, will be carried out. No special beam condition is required in this tuning phase.

During the dedicated operation time, RHICf will change its vertical position according to Fig.2.2. Because this causes an unstable response of ZDC behind the RHICf detector, luminosity determination of PHENIX must be carried out using other channels. As shown in Tab.2.1, the RHICf acceptance depends on the vertical detector position. Assuming a luminosity live-time about 8 hours, though this may be longer with $\beta^*=10$ m, a few sets of 30 min runs for each position will be performed in a single fill (delivered luminosity is $20 \text{ nb}^{-1}/30 \text{ min}$ with a peak luminosity). Since DAQ speed is limited anyway at 1 kHz, 1.4 M events at each position are obtained after taking account of 20% inefficiency in the analysis. Assuming a single shower prescaling at 800 Hz (800 Hz/28 kHz=3%) and 70% neutron detection efficiency, statistics in each event category are shown in Tab.3.2 according to the acceptance in Tab.2.1. Corresponding effective integrated luminosities (and number of inelastic collisions) are 0.5 nb^{-1} (2.4×10^7) and 16 nb^{-1} (8×10^8) for single shower events and π^0 events, respectively. Detailed studies such as expected observed spectra and sensitivity to the asymmetry measurements with reasonable binnings are given in Chap.4.

Table 3.2: Expected event statistics in 30 min of operation at $L=1.1 \times 10^{31}$. A prescaling of single shower events (photons and neutrons) to 800 Hz, 70% neutron detection efficiency and 20% offline event reduction are assumed. TS and TL designate Small Tower (calorimeter) and Large Tower, respectively.

Position	All event	photon		neutron		π^0
		TS	TL	TS	TL	
0	1.3M	240k	330k	290k	290k	180k
1	1.4M	220k	350k	260k	320k	200k
2	1.3M	250k	330k	300k	270k	160k
3	1.3M	280k	360k	270k	250k	120k
4	1.2M	300k	370k	250k	230k	90k
5	1.2M	370k	330k	270k	190k	50k

In addition to the position scan for physics, some surveys for the detector response, gain, threshold, trigger logic, will be performed. It is also planned to repeat short operations at position 0 to monitor the ‘zero’ degree position. Including these surveys we require one day of RHICf physics operation. For contingency, one more

day of operation time is requested.

Chapter 4

Expected results

4.1 Single particle spectra

With 2 hour of data taking a dataset corresponding to an effective integrated luminosity of 2 nb^{-1} or 1×10^8 inelastic collisions is obtained for single shower events. Expected photon and neutron spectra with 10^8 collisions taken at each of 6 scan positions (12 hours) are shown in Fig.4.1 and Fig.4.2, respectively. The results for 4 rapidity bins $6.26 < \eta < 6.49$, $6.87 < \eta < 7.40$, $7.40 < \eta < 7.83$ and $8.27 < \eta$ are presented as examples. In the calculation, event generators PYTHIA 8.185 [21], EPOS LHC [24] and QGSJET II-03 [6] are used. Only statistical errors are indicated in the plots. Neutron spectra after taking into account the 70% detection efficiency, 40% energy resolution and 1 mm position resolution are shown in Fig.4.3. A possible improvement of the energy resolution by a joint analysis with the ZDC is not considered in these plots. In any cases, except at the highest energy bins, statistical errors are small enough that the differences between models will be clearly evident. Since the uncertainty will be dominated by possible systematic errors, a careful studies of detector performance and beam condition are necessary. An advantage of the RHICf measurements is that the performance of the detector have been studied at the CERN SPS beam line using 100-350 GeV proton [25] and 100-250 GeV electron [26] beams coinciding with the energy range at RHIC.

4.2 π^0 spectra

With 30 min of data taking, a dataset corresponding to an effective integrated luminosity 16 nb^{-1} or 8×10^8 inelastic collisions is obtained. Expected π^0 spectra with 10^8 collisions, corresponding to 4 min (this is limited by the CPU time in simulation), at $6.04 < y < 6.16$, $6.36 < y < 6.70$, $6.70 < y < 6.88$ and $7.25 < y < 7.62$ are shown in Fig.4.4 where y is rapidity of π^0 . In the calculation, event generators PYTHIA 8.185, EPOS LHC and QGSJET II-03 are used. Only statistical errors are indicated in the plots. With this MC statistics, the statistical errors are at the 10% level for each bin. With a reasonable data taking time, we can expect the statistical errors to be well below the systematic uncertainties. The differences between models are clearly evident

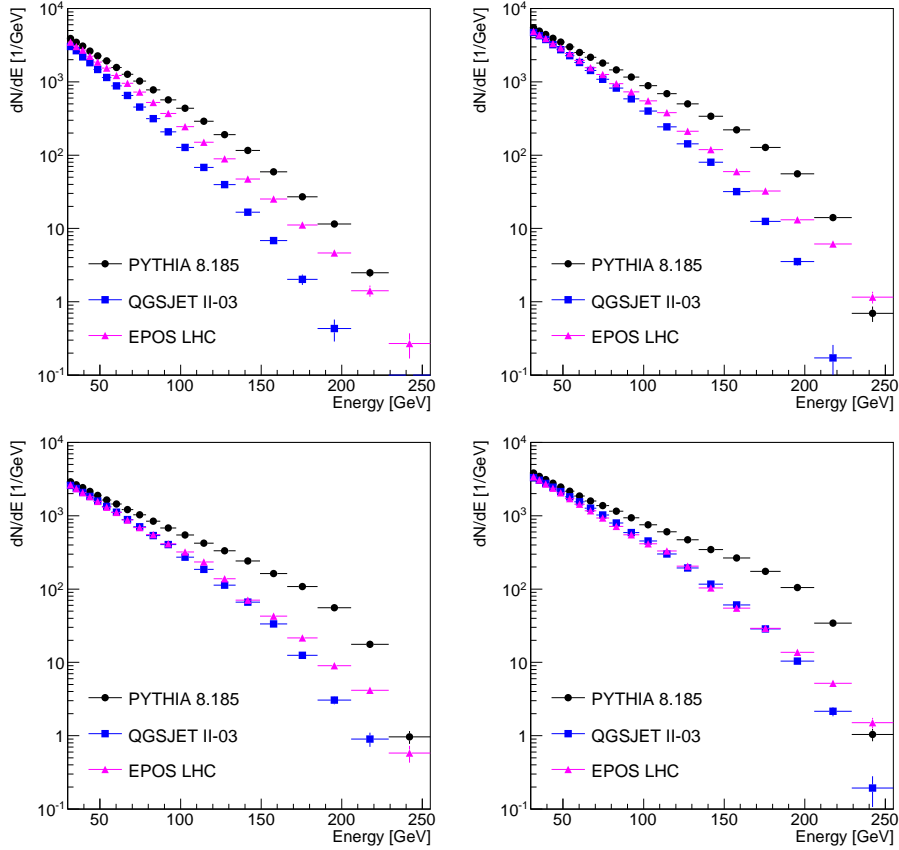


Figure 4.1: Energy spectra of photons expected from a 2 hours \times 6 positions dataset at $6.26 < \eta < 6.49$ (top-left), $6.87 < \eta < 7.40$ (top-right) $7.40 < \eta < 7.83$ (bottom-left) and $8.27 < \eta$ (bottom-right). Different colors designate event generators used in the calculation.

already with the statistics obtained from the short data taking.

4.3 Spin asymmetry

Using the same data set to the spectrum analysis, RHICf can study the spin asymmetry like PHENIX but with a better position resolution and hence a better p_T resolution than the PHENIX SMD. The vertical scan allows RHICf to cover up to higher p_T than PHENIX. Expected numbers of events with $x_F > 0.4$ in several p_T bins are summarized in Tab.4.3. Effective number of collisions (luminosity) of 10^8 (2 nb^{-1}) and 10^9 (20 nb^{-1}) at each of 6 positions are assumed for the single shower events (neutrons and photons) and π^0 events, respectively. These correspond to a data taking time of 12 and 4 hours, respectively, and can be completed during the spectral measurements discussed in Sec.4.1. Statistical accuracies for determining the amplitude of asymmetry (δA) are also summarized in the table. Assuming a polarization P to be 50%, δA is defined as $1/(P\sqrt{N})$. According to these statistics,

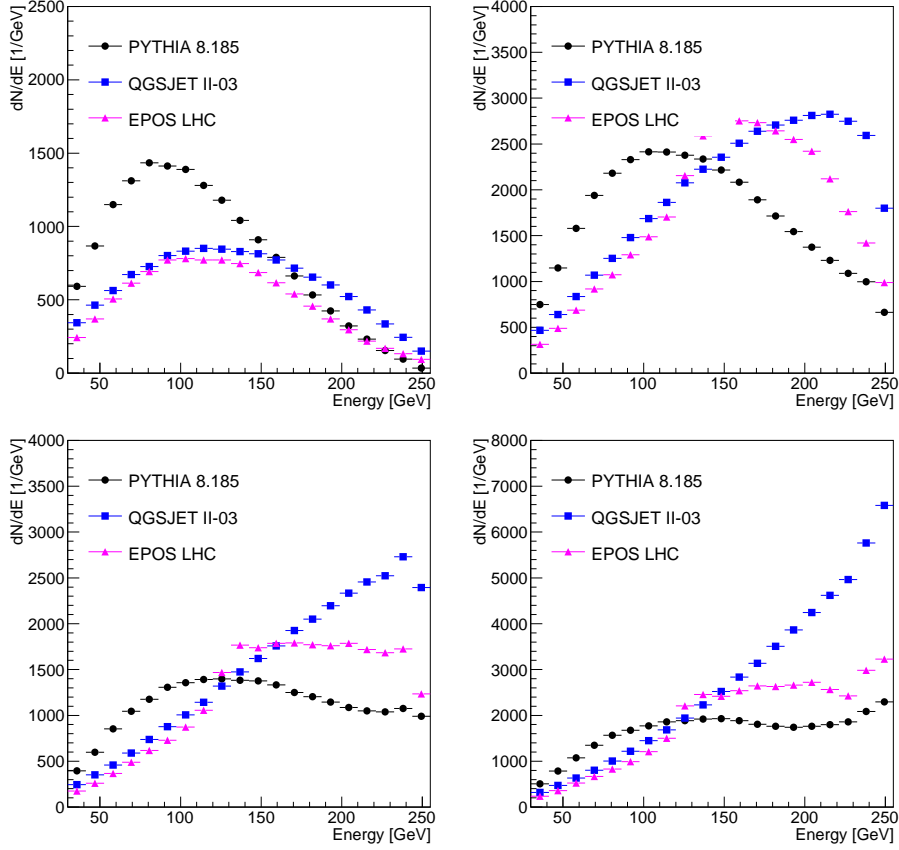


Figure 4.2: Energy spectra of neutrons expected from a 2 hours \times 6 positions dataset at $6.26 < \eta < 6.49$ (top-left), $6.87 < \eta < 7.40$ (top-right) $7.40 < \eta < 7.83$ (bottom-left) and $8.27 < \eta$ (bottom-right). Different colors designate event generators used in the calculation.

$\sim 1\%$ statistical accuracy is obtained at $p_T < 1.0$ GeV/c, 0.5 GeV/c and 0.5 GeV/c for neutrons, photons and π^0 , respectively. These extend the past PHENIX measurements with good overlapping p_T coverages. Expected data points given by RHICf overlaid on the past PHENIX result are shown in Fig.4.5 as red ellipses. Here the sizes of the ellipses indicate the expected p_T resolution of RHICf [22] and $\pm 1\%$ errors on asymmetry.

There are some options under consideration for the asymmetry measurements.

- High energy enhanced trigger to increase the statistics of high energy (high p_T) events.
- Trigger using the PHENIX Beam Beam Counter (BBC) as was done in the PHENIX analysis.

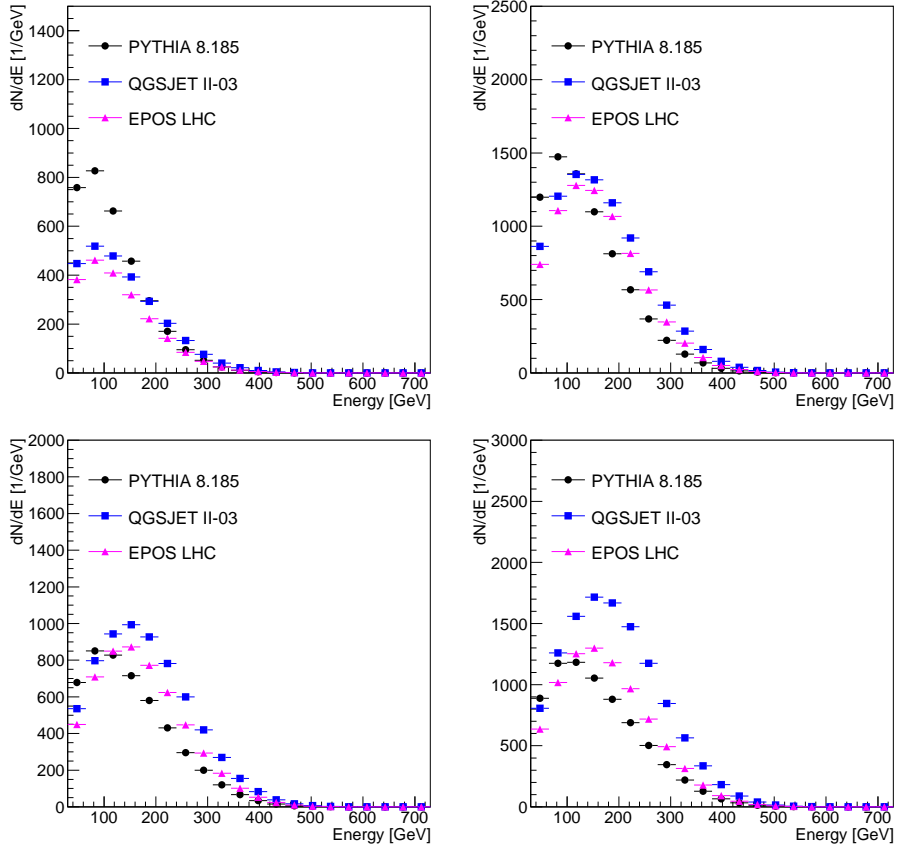


Figure 4.3: Energy spectra of neutrons expected from a 2 hours \times 6 positions dataset at $6.26 < \eta < 6.49$ (top-left), $6.87 < \eta < 7.40$ (top-right) $7.40 < \eta < 7.83$ (bottom-left) and $8.27 < \eta$ (bottom-right). Effects of detection efficiency, energy resolution and position resolution of the RHICf detector are taken into account. Different colors designate event generators used in the calculation.

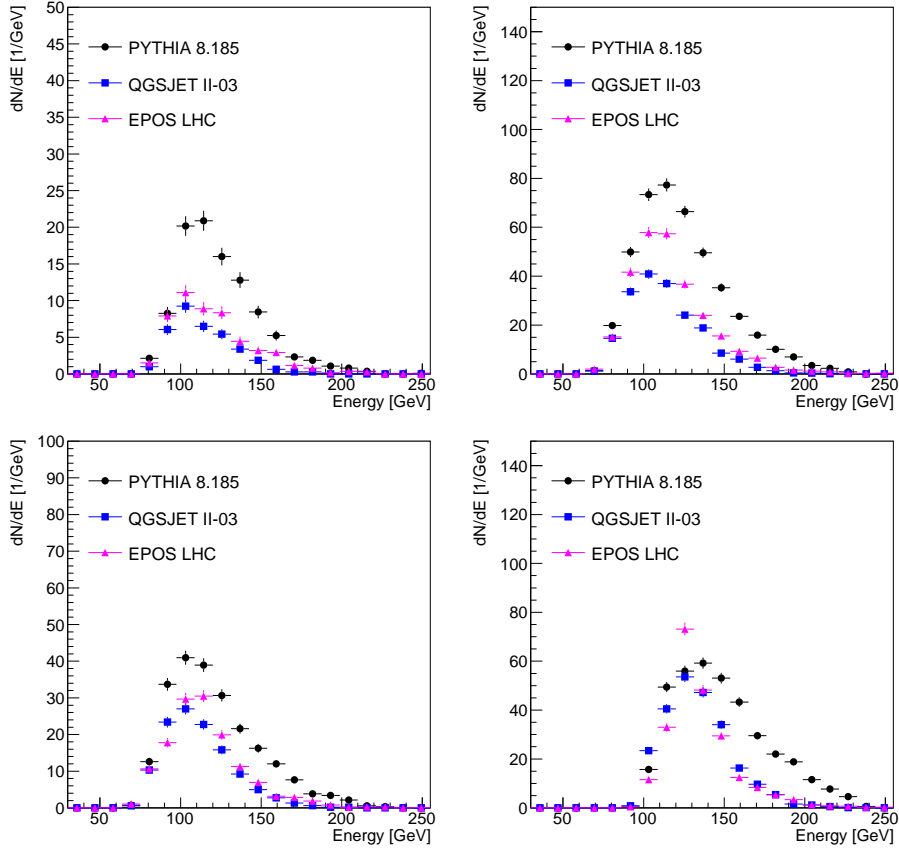


Figure 4.4: Energy spectra of π^0 expected from a $4 \text{ min} \times 6$ positions dataset at $6.04 < y < 6.16$ (top-left), $6.36 < y < 6.70$ (top-right), $6.70 < y < 6.88$ (bottom-left) and $7.25 < y < 7.62$ (bottom-right). Different colors designate event generators used in the calculation.

Table 4.1: Statistics (1,000 events) obtained from 12 nb^{-1} (12 hours) and 120 nb^{-1} (4 hours) effective luminosities for single shower events (neutron and photon) and π^0 events, respectively with $x_F > 0.4$. δA indicates the expected statistical accuracy of the asymmetry determination.

p_T (GeV/c)	neutron		photon		π^0	
	$N(\times 10^3)$	δA	$N(\times 10^3)$	δA	$N(\times 10^3)$	δA
0.0 – 0.1	660	0.0025	110	0.0060	100	0.0063
0.1 – 0.2	920	0.0021	120	0.0058	130	0.0055
0.2 – 0.3	820	0.0022	110	0.0060	89	0.0067
0.3 – 0.4	670	0.0024	79	0.0071	58	0.0083
0.4 – 0.5	450	0.0030	43	0.0096	37	0.010
0.5 – 0.6	250	0.0040	18	0.015	14	0.017
0.6 – 0.8	170	0.0049	8	0.022	8	0.022
0.8 – 1.0	29	0.012	1	0.063	1	0.063

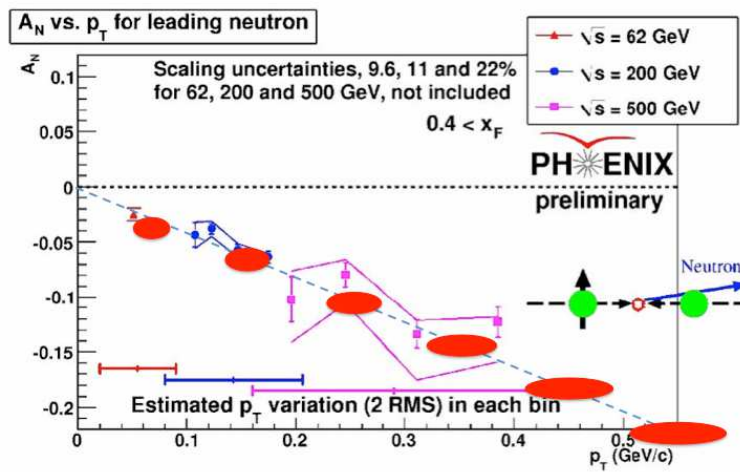


Figure 4.5: Expected RHICf result for neutron asymmetry is plotted as red ellipses on the past PHENIX result. RHICf p_T resolution and $\pm 1\%$ errors are indicated by the size of the ellipses.

Chapter 5

Schedule and expected supports from BNL

5.1 Schedule

Detector

LHCf will finish its operation at LHC in early May 2015. Then the detector will be removed from the tunnel during a technical stop in June. Because a weak activation is expected at the time of removal, a few weeks of cooling at the CERN site is necessary. The arrival of the detector at BNL will be around October. After a checkout of the detector condition at BNL, it will be installed in RHIC.

DAQ and mechanical setup

Before the detector installation in 2015 autumn, we need to perform

- Cabling from RHICf installation slot to the rack room
- Construction of the detector support structure
- Mockup test for detector installation
- Setup of the electronics in the rack room
- Setup of the counting room
- Dry run of the data taking, synchronization with accelerator and PHENIX

A time line of the preparation is shown in Fig.5.1. Grey and black items indicate the major activities related to LHCf. Blue items show the activities carried out without the detector that can be proceeded immediately after the approval of this proposal. The schedule of the detector transport after the LHCf operation is drawn by orange and the RHICf physics operation is indicated by red. The timing of the final operation depends on the actual scheduling of RUN16, but here the operation at the end of RUN16 is supposed.

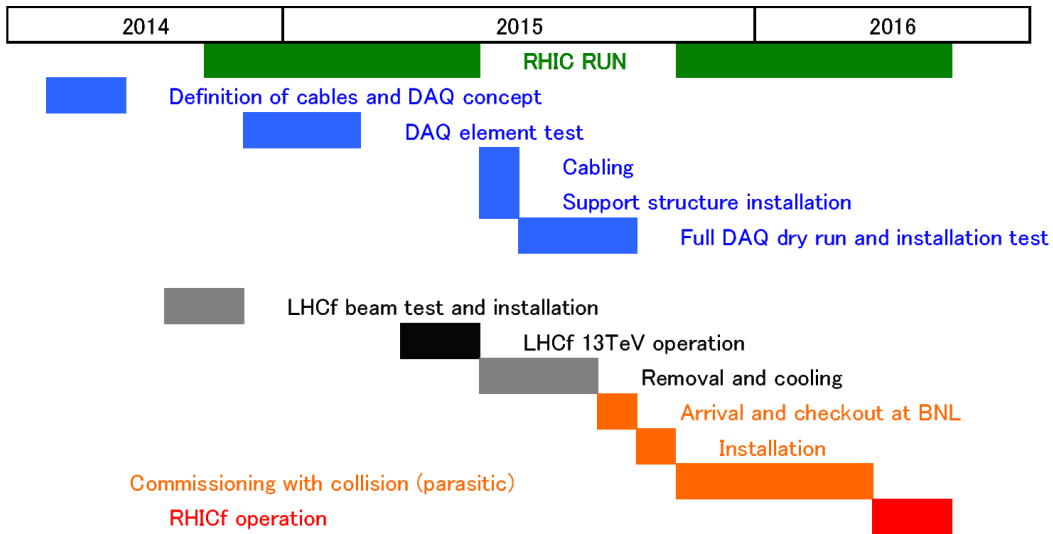


Figure 5.1: Schedule until RHICf operation

5.2 Expected supports from BNL

Some technical supports including man power from BNL and/or PHENIX are expected to prepare the experiment. They are listed up below.

- Cabling from the RHICf installation slot to the PHENIX rack room
- Construction and installation of the detector support structure
- Transportation, installation and geometrical survey of the detector
- Support for custom process not to delay the detector arrival from CERN

The cost is supposed to be covered by the RHICf collaboration.

Chapter 6

Manpower and budget

The project is carried out mainly by Nagoya university, Waseda university and RIKEN in Japan and University of Florence, University of Catania and INFN in Italy. Addition to the authors in this proposal, some graduate students will participate to this experiment to write their PhD theses. All members including students are trained enough in the PHENIX and the LHCf experiments to carry out the RHICf project efficiently.

Because the detector and the major electronics are already available, not large amount of budget is required. The major items are

- Travel cost between Japan/Italy and BNL (approx. 100 k USD)
- Updating the electronics (approx. 20 k USD)
- Cost for cables and cabling work (approx. 10 k USD)
- Construction of detector support (approx. 5 k USD)
- Transport of the material from CERN to BNL (approx. 5 k USD)

The cost can be manageable within the running budget of the member institutes and also grants now being applied. The approval of this proposal will help to obtain dedicated grants for the RHICf program.

Bibliography

- [1] The Pierre Auger Collaboration, PRL, 104, 091101 (2010); The Pierre Auger Collaboration, PLB, 685, 239-246 (2010).
- [2] The Telescope Array Collaboration, Astropart. Phys., 39-40, 109-119 (2012); The Telescope Array Collaboration, International Symposium on Future Directions in UHECR Physics (2012).
- [3] W.D. Apel, *et al.*, Astropart. Phys., **31**, 86-91 (2009).
- [4] D. d'Enterria *et al.*, Astropart. Phys., **35**, 98-113 (2011).
- [5] F.W. Bopp, J. Ranft, R. Engel, S. Roesler, *Phys. Rev. C* **77**, 014904 (2008).
- [6] S. Ostapchenko, *Phys. Rev. D* **74**, 014026 (2006).
- [7] The STAR Collaboration, Phys. Rev. Lett, **97**, 152302 (2006).
- [8] The ALICE Collaboration, CERN-PH-EP-2012-306 (2012).
- [9] Y. Fukao *et al.*, Phys. Lett. **B650**, 325-330 (2007). [hep-ex/0610030].
- [10] The PHENIX Collaboration, PRD, **88**, 032006 (2013).
- [11] The PHENIX Collaboration, J. Phys. Conf. Ser., **295**, 012097 (2011).
- [12] B. Z. Kopeliovich, I. K. Potashnikova, I. Schmidt and J. Soffer, Phys. Rev. D **84**, 114012 (2011).
- [13] The LHCf Collaboration, Technical Design Report, CERN-LHCC-2006-004 (2006).
- [14] The LHCf Collaboration, IJMPA, **28**, 1330036 (2013).
- [15] The LHCf Collaboration, Phys. Lett. **B715**, 298-303 (2012).
- [16] The LHCf Collaboration, Phys. Lett. **B703**, 128-134 (2011).
- [17] The LHCf Collaboration, Phys. Rev. **D86**, 092001 (2012).
- [18] The LHCf Collaboration, arXiv:1403.7845v1 [nucl-ex]
- [19] The LHCf Collaboration, JINST, **3**, S08006 (2008).

- [20] O.Adriani et al., JINST, **5**, P01012 (2010).
- [21] T. Sjostrand, S. Mrenna and P. Skands, Comput. Phys. Comm., **178**, 852 (2008).
- [22] Y.Itow et al., arXiv:1401.1004v1 [physics.ins-det]
- [23] W. Fischer et al., "RHIC Collider Projections (FY 2014 ? FY 2018)," 6 April 2014
- [24] K. Werner, F.-M. Liu, T. Pierog, *Phys. Rev. C* **74**, 044902 (2006).
- [25] K.Kawade et al., JINST, **9**, P03016 (2014).
- [26] T. Mase et al., Nucl. Instrum. Meth.,**A671** 129-136 (2012).